Int J Clin Exp Pathol 2016;9(6):5837-5848
www.ijcep.com /ISSN:1936-2625/IJCEP0026524

Original Article

Simvastatin suppresses cell migration and invasion, induces G0/G1 cell cycle arrest and apoptosis in osteosarcoma cells

Hongliang Wang[1], Na Sun[2], Xin Li[1], Ka Li[1], Jiguang Tian[3], Jianmin Li[1]

Departments of [1]Orthopedics, [3]Emergency, Qilu Hospital, Shandong University, Ji'nan, Shandong, China; [2]Shandong Institute of Medicine and Health Information, Ji'nan, Shandong, China

Received February 23, 2016; Accepted May 21, 2016; Epub June 1, 2016; Published June 15, 2016

Abstract: Simvastatin has been reported to possess anti-cancer activities. However, the roles and molecular mechanisms of simvastatin in osteosarcoma progression are still unknown. In this study, we investigated the effects of simvastatin on cell proliferation, migration and invasion, cell cycle and apoptosis in MNNG/HOS osteosarcoma cells. Our present study demonstrated that simvastatin inhibited osteosarcoma cell proliferation in culture and tumor growth in vivo. Simvastatin suppressed MNNG/HOS cells migration and invasion by down-regulation of expressions of MMP-2 and -9. Simvastatin induced MNNG/HOS cells G0/G1 phase arrest via down-regulation of cyclin D1, CDK2, CDK4 as well as up-regulation of p21 and p27. Simvastatin induced MNNG/HOS cells apoptosis through inactivation of PI3K/Akt signaling pathway. Simvastatin can partly approach the efficacy of LY294002 and completely reverse the IGF-1-induced activation of PI3K/Akt signaling pathway. Overall, our novel findings suggested the possibility of simvastatin as a tumor suppressor for human osteosarcoma treatment.

Keywords: Osteosarcoma, simvastatin, cell cycle arrest, apoptosis, PI3K/Akt pathway

Introduction

Osteosarcoma is the most common primary tumor of bone in children and young adults. Because these tumors have a high propensity to metastasis, most often to the lung, they are ranked among the most frequent causes of cancer-related death, despite the fact this cancer type only accounts for 5-6% of all childhood tumors [1]. Osteosarcoma can transpire in any bone, mostly are found near the metaphyseal growth plates of the long bones, especially the distal femur, proximal tibia and proximal humerus [2]. The current favored treatment for Osteosarcoma involves neoadjuvant chemotherapy, followed by surgery and chemotherapy again. Although surgical techniques and chemotherapeutic strategies have been improved during the past few years, the 5-year survival rate of Osteosarcoma patients has not significantly increased. Thus, there is a great need to develop more effective treatments for this deadly disease.

Statins, which are competitive inhibitors of 3-hydroxy-3-methylglutaryl coenzyme A reductase (HMGCR), have been widely prescribed for the treatment of hypercholesterolemia and are among the most widely used pharmaceutical agents in the world. These drugs effectively lower circulating cholesterol levels by decreasing the intracellular synthesis of cholesterol, and extensive clinical trials have demonstrated that statins reduce the risk of myocardial infarction, ischemic stroke, and the development of peripheral arterial disease [3]. Recently, statins have received more attention for their anticancer effects. Evidence is accumulating that statins exert the tumor cytotoxicity through the inhibition of cell proliferation, induction of apoptosis, or inhibition of angiogenesis [4-6]. Of all statins, Simvastatin (Sim), a lipophilic member, have showed more potent anti-tumor activity in vitro and in vivo in previous studies [7]. Numerous experimental data confirmed that Sim inhibits a variety of cancer cells growth, including ovarian cancer [8], bile duct cancer

[9], renal cancer [10], prostate cancer [11] and hepatic cancer [12]. Evidence is mounting to support claims that Sim exert the anti-tumor effects by inducing apoptosis and inhibiting cell cycle progression through a variety of cell signaling pathways [8, 9, 12, 13]. However, there is little research referred to the effects of Sim on human osteosarcoma cells as well as molecular mechanisms. Thus, in the present study, the effects of Sim on osteosarcoma and possible molecular mechanisms were further studied. Our findings demonstrated that Sim could inhibit the human osteosarcoma cells proliferation in vitro and in vivo through multimechanisms, implying that Sim may be a promising therapeutic drug for osteosarcoma patients.

Materials and methods

Chemicals and reagents

Sim (Sigma-Aldrich Chemical Co, St. Louis, MO, USA) was obtained as solid powder and dissolved in 100 mg/ml solution of DMSO (Sigma-Aldrich Chemical Co, St. Louis, MO, USA) and then diluted with the medium to the desired concentration prior to use. Final DMSO concentration was lower than 0.1% and has been verified not to interfere with the test system employed. Cell counting kit (CCK)-8 was purchased from Dojindo Molecular Technologies Inc. (Kumamoto, Japan). Annexin V-FITC and propidium iodide (PI) double staining kit was obtained from Nanjing Kaiji Biotechnology Co. Ltd. (Nanjing, China). Insulin-like growth factor-1 (IGF-1) was obtained from PeproTech China (Suzhou, China). LY294002 (the PI3K inhibitor) were purchased from Cell Signaling Technology (Beverly, MA, USA). All other chemicals and reagents were commercially available and of standard biochemical quality.

Cell line and culture

Human osteosarcoma cell line MNNG/HOS were obtained from ATCC (Rockville, MD, USA). The cells were cultured in Dulbecco's modified Eagle's medium (DMEM) (Invitrogen, Carlsbad, CA, USA) containing 10% fetal bovine serum (Invitrogen, Carlsbad, CA, USA) in a humidified incubator with 5% CO_2 at 37°C.

Cell viability assay and morphological observation

Cell viability was determined using a cell counting kit (CCK)-8 assay. The MNNG/HOS cells were seeded in 96-well plates at 1×10^4 cells per well in 100 µl culture medium. After overnight incubation, The cells were then subjected to different concentrations (0.5, 1, 2, 4, 8, 16, 32, 64 µM) of Sim for 24, 48 and 72 h. Cells grown in DMEM containing an equivalent amount of DMSO without any compound treatment functioned as control. 10 µl CCK-8 was added into the culture well after the DATS treatment and then the cells were incubated for 2 h at 37°C with 5% CO_2 in a humidified incubator, and the viability of the cells was measured by absorption at 490 nm using an ELISA reader (BioTek, Winooski, VT, USA). Inhibitory ratio (%) = (OD control-OD treated)/OD control × 100%. For assessment of cell morphology of MNNG/HOS cells after exposed to Sim, a total of 4×10^5 cells/well were cultured in 6-well plates at 37°C overnight, and then each well were treated with 0, 8, 16 µM Sim for 48 h. The cells in each well were examined under a phase-contrast microscope and then were photographed (Olympus, Melville, NY).

Cell migration and invasion assays

Cell migration (wound-healing) assay was conducted to determine the capacity of cell migration. Briefly, the wound was generated when the cells reached around 90% confluency by scratching the surface of the plates with a pipette tip. The cells were incubated in different concentrations (0, 8, 16 µM) of Sim for 48 h respectively, and then photographed at the identical location of the initial image with an Olympus Optical microscope (Olympus, Melville, NY). The percentages of open spaces covered by migrated cells were determined as described previously [14]. The determinations of invasion assay was performed through 24-well Transwell Insert (8 µm pore filters; Corning, NY, USA) coated with Matrigel (BD Biosciences, Bedford, MA, USA) according to manufacturer's protocol. Initially, the MNNG/HOS cells were cultured for 24 h in serum-free DMEM, and then cells were placed in the upper chamber of the Transwell Insert (1×10^4 cells/200 µl medium) and treated with desired concentration of Sim (0, 8, 16 µM). The 600 µl complete medium containing 10% FBS was placed in the lower chamber. After 48 h of incubation, the cells in the upper chamber were removed with a cotton swab, and the cells, which invaded through the Matrigel, were then fixed with 4% formaldehyde and stained with 2% crystal violet. Finally, the cells in the

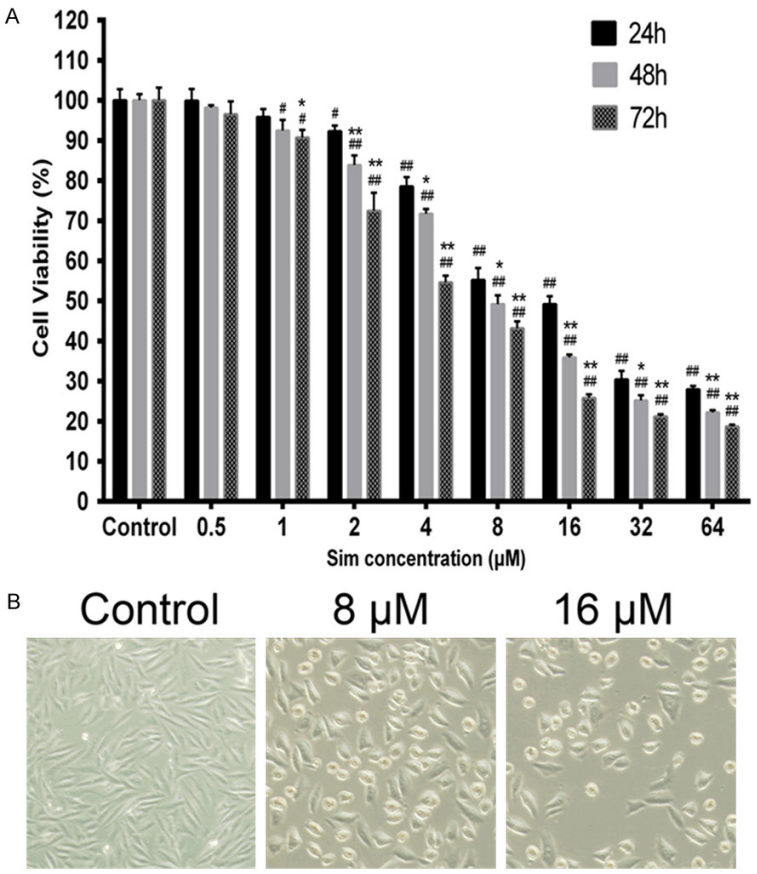

Figure 1. Effects of Sim on the cell growth of MNNG/HOS cells. A. MNNG/HOS cells were treated with 0.5, 1, 2, 4, 8, 16, 32, 64 μM μM of Sim for 24, 48 and 72 h. The cell growth inhibitory rate was measured using CCK-8 assay. The results from three independent experiments are represented in the form of means ± SD. #P<0.05, ##P<0.01 compared with control groups. *P<0.05, ** P<0.01 compared with 24 h groups. B. Representative morphologies of MNNG/HOS cells respectively under phase contrast microscopy (magnification, x100).

lower surface of the filter which penetrated were counted and photographed under a phase-contrast microscope. Abilities of invasion were quantified by counting the number of invaded cells from six random microscopic fields [15].

Cell cycle analysis

The MNNG/HOS cells at a density of 3×10^5 cells/well were plated in 6-well plates for overnight incubation and then were treated with different concentrations (0, 8, 16 μM) of Sim for 48 h. Both floating and attached cells were collected and washed in ice-cold PBS, resuspended, and fixed with 70% ice-cold ethanol overnight at 4°C. Then the cells were centrifuged and treated with RNase A (20 μl in 500 μl PBS) for 30 min at 37°C. Subsequently, the cells were added 400 μl PI and incubated at room temperature for 30 min in the dark. Cell cycle distribution was analyzed using flow cytometer (BD Calibur). Data analysis was performed using FlowJo software.

Cell apoptosis assay

The apoptosis of MNNG/HOS cells was examined by flow cytometry using Annexin V-FITC/PI staining. Briefly, the cells were cultured in 6-well plates (3×10^5 cells/well) overnight and then were treated with indicated concentrations (0, 8, 16 μM) of Sim for 48 h. Both attached and floating cells were accumulated and washed twice with ice-cold PBS, resuspended in 500 μl binding buffer. The samples were added 5 μl Annexin V-FITC and 5 μl PI, and incubated at room temperature for 15 min in the dark. Cell apoptosis was analyzed using flow cytometer (BD Calibur). Data analysis was performed using FlowJo software.

Western blot analysis

For the preparation of cytosolic extracts, the MNNG/HOS cells were lysed in RIPA with 1 mM PMSF for 30 min on ice. The mixture was centrifuged at 14,000 g for 5 min and the precipitate was discarded. Protein concentration was measured with BCA protein assay kit (Beyotime, Haimen, China). Samples containing equal amount of protein were separated by SDS-PAGE, and then transferred to polyvinylidene fluoride (PVDF) membranes (Merck Millipore, MA, USA) using standard procedure. The PVDF membrane was blocked in 5% (w/v) skim milk powder in Tris-buffered saline containing 0.1% Tween-20 for 2 h at room temperature. The primary antibodies against GAPDH (Abcam, ab-

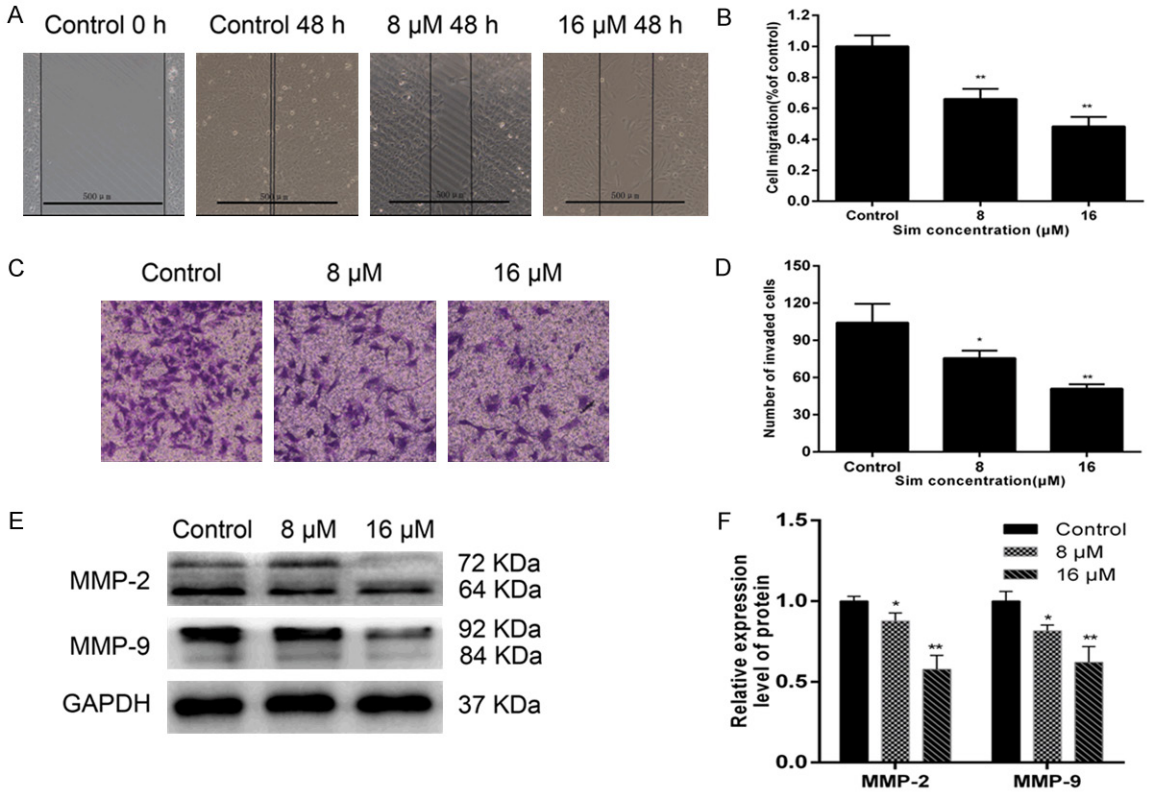

Figure 2. Sim suppressed cell migration and invasion and down-regulated the expression of MMP-2 and -9 after MNNG/HOS cells were treated with different concentrations of Sim for 48 h. A and B. The effects of Sim on the migration ability of cells were determined by wound healing assay. Cell migration was assessed by the percentages of original open spaces covered by migrated cells. C and D. The effects of Sim on the invasive ability of cells were determined by Transwell assay. Images of the cells that invaded through the Matrigel to the lower chamber at 48 h were captured by light microscopy (magnification, ×100). Columns indicated the mean numbers of MG63 and MNNG/HOS cells that invaded through the Matrigel from six random microscopic fields. E and F. Expression levels of MMP-2 and -9 detected by Western blot in MNNG/HOS cells treated with Sim. GAPDH was used as a loading control. Data are expressed as the mean ± SD from three independent experiments. *P<0.05, **P<0.01 vs. control groups.

9485), PI3K (p110β) (Abcam, ab32569), Akt (Cell Signaling Technology, #9272), p-Akt (Ser-473) (Cell Signaling Technology, #9271), Bax (Abcam, ab32503), Bcl-2 (Cell Signaling Technology, #2870), cleaved PARP (Abcam, ab32-064), cyclin D1 (Cell Signaling Technology, #29-78), CDK2 (Abcam, ab32147), CDK4 (Abcam, ab108355), p21 Cip1 (Abcam, ab7960), p27 Kip1 (Abcam, ab7961), MMP-2 (Cell Signaling Technology, #4022), and MMP-9 (Cell Signaling Technology, #3852) were diluted according to the instructions of antibodies and incubated overnight at 4°C. Then the horseradish peroxidase (HRP)-conjugated secondary antibodies against rabbit IgG (Zhongshanjinqiao Biotechnology Co., Ltd, Beijing, China) were added at a dilution ratio of 1:5000 and incubated at room temperature for 2 h. The blots were visualized using an enhanced chemiluminescence (ECL) detection kit (Merck Millipore, Billerica, MA, USA) according to the manufacturer's instructions. The relative protein expression levels were then determined using ChemiDoc Touch Imaging System (Bio-Rad Laboratories, Inc., CA, USA) and quantified by Image Lab and ImageJ software. In order to quantify changes to protein expression, the target protein was normalized against GAPDH.

In vivo xenograft tumor assay

The MNNG/HOS cells were counted by trypan blue staining. Then the cells (5×10^6 cells) were suspended in non-serum medium with equal volume of Matrigel (BD Biosciences) and inoculated subcutaneously into the right flank of

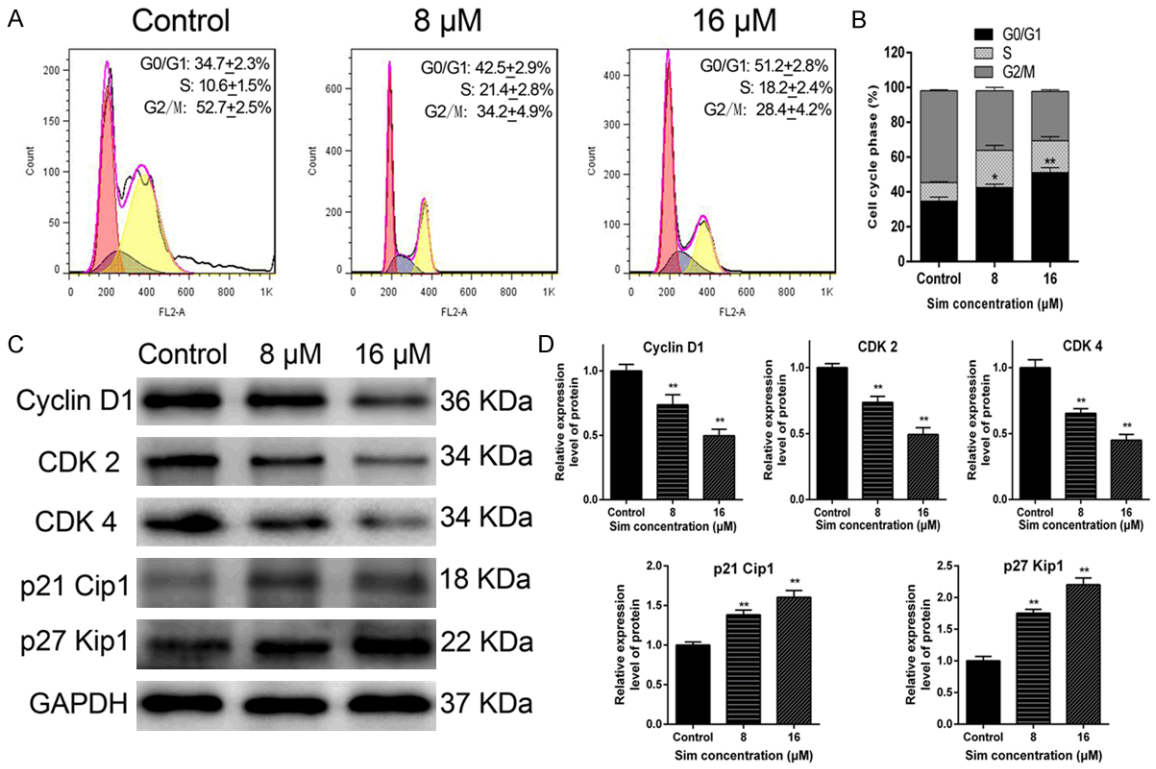

Figure 3. Effects of Sim on cell cycle distribution and the expressions of cell cycle related proteins in MNNG/HOS cells. After treatment with Sim at 0, 8, 16 μM for 48 h, A. cell cycle distribution was determined by flow cytometric analysis. B. The percentage of cells in various phases of cell cycle. Data are expressed as the means ± SD from three independent experiments. C and D. Expression levels of cyclin D1, CDK2, CDK4, p21 Cip1 and p27 Kip1 were detected by Western blot in Sim treatment MNNG/HOS cells. GAPDH was used as a loading control. Data are expressed as the means ± SD from three independent experiments. *P<0.05, **P<0.01 vs. control groups.

nude mice. Sixteen mice were injected with the MNNG/HOS cells and then randomly divided into the control and simvastatin groups. The Sim treatment (intraperitoneal injection, 3 mg/kg/day) was initiated twelve days after the inoculation, and tumor volume was measured every week using palpation until tumors had grown to a size amenable to caliper measurement. Control mice were given the same volume of normal saline. The body weight of mice in both groups was also measured every week. Tumor volume was calculated using the following equation (width^2 × length)/2. About 7 weeks after inoculation, mice were euthanized by subcutaneous injection with sodium pentobarbital (40 mg/kg) and the tumor volume was calculated. This study was performed with approval from the Animal Ethics Committee of Qilu Hospital. All surgeries were performed under sodium pentobarbital anesthesia (Sigma, St. Louis, MO, USA), and all efforts were made to minimize suffering.

Statistical analysis

All the experiments were performed three times independently. All the results were expressed as the mean ± SD. The Student's t-test by GraphPad InStat software (GraphPad Software, Inc., San Diego, CA, USA) was used to compare the difference among different groups. A P< 0.05 was considered statistically significant.

Results

Effect of Sim on MNNG/HOS cell proliferation

The anti-proliferative effect of Sim (**Figure 1A**) against MNNG/HOS cells was examined by CCK-8 assay. Our data showed that Sim significantly inhibited MNNG/HOS cell proliferation in a dose- and time-dependent manner (P<0.05). The IC_{50} values of Sim at 24, 48, 72 h were 15.10±2.08, 9.91±1.05, 6.24±0.83 μM respectively. For the morphological changes of MNNG/HOS cells after incubation with Sim at

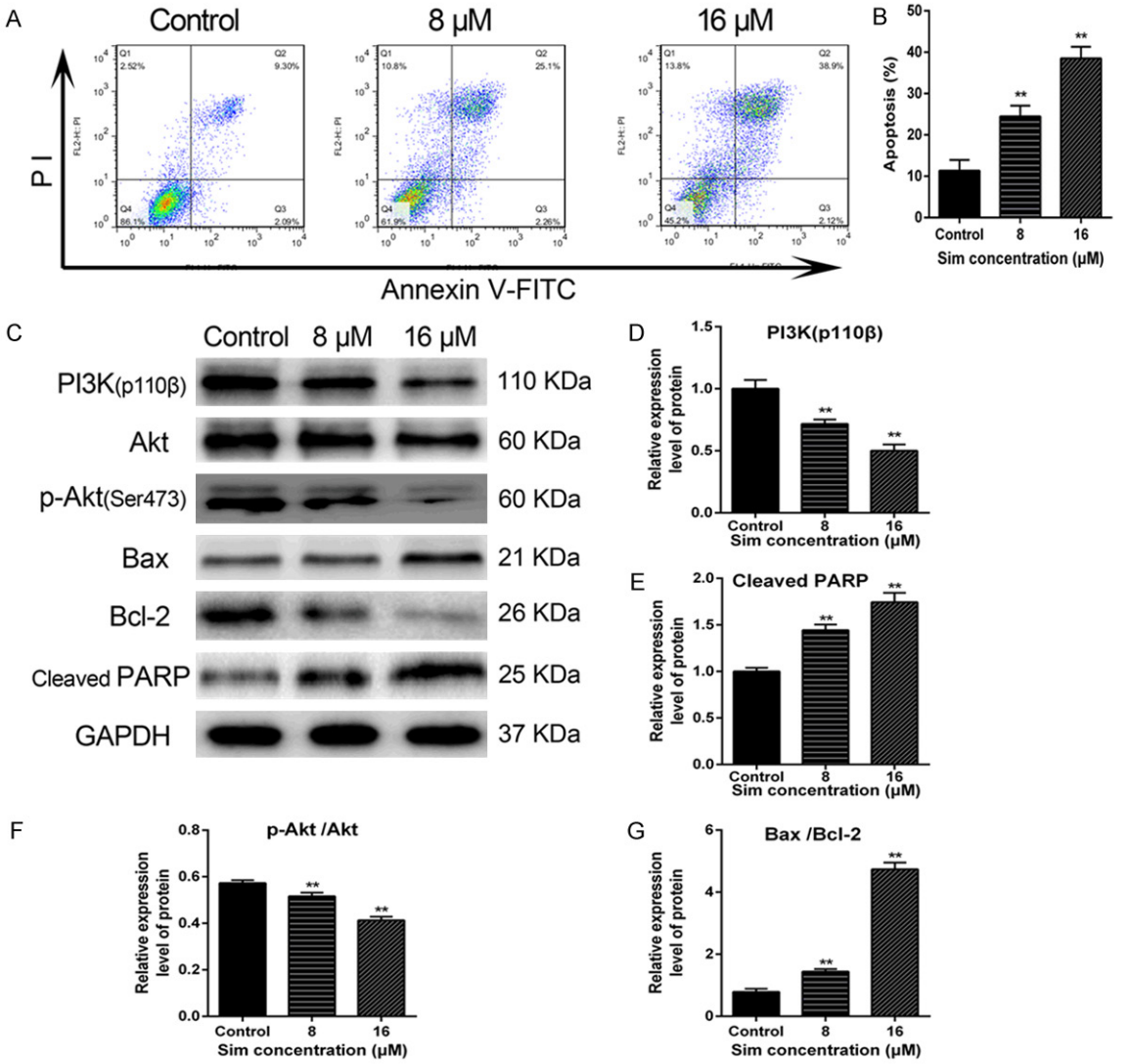

Figure 4. Sim induced MNNG/HOS cells apoptosis and inactivation of the PI3K/Akt signaling pathway. After Sim treatment at 0, 8, 16 μM for 48 h, the MNNG/HOS cells were stained with Annexin V-FITC and PI for flow cytometric analysis and protein expression levels were determined by Western blot. (A) Flow cytometric analysis. (B) The percentage of apoptotic cells (early apoptosis + late apoptosis). (C) Representative blots. Relative expression levels of (D) PI3K (p110β), (E) cleaved PARP. The ratio of expressions of (F) p-Akt/Akt, (G) Bax/Bcl-2. GAPDH was used as a loading control. Data are expressed as the means ± SD from three independent experiments. *P<0.05, **P<0.01 vs. control groups.

different concentrations (0, 8, 16 μM) for 48 h, the control group cells showed a typical polygonal and intact appearance, whereas the Sim-treated cells displayed dose-dependent changes in cell counts, cell shrinkage, loss of cell to cell contact, poor adherence and floating shapes (**Figure 1B**, magnification, x100).

Sim suppressed cell migration and invasion

After the MNNG/HOS cells were treated with Sim at 0, 8, 16 μM for 48 h, the wound healing assay showed that Sim significantly suppressed the migration ability of MNNG/HOS cells in a dose-dependent manner compared with the control groups (**Figure 2A** and **2B**, P<0.01). Transwell assay showed that DATS significantly reduced the invasive ability of MNNG/HOS cells in a dose-dependent manner compared with the control groups (**Figure 2C** and **2D**, P<0.05). Collectively, our results suggested that Sim played a suppressive role in MNNG/HOS cells migration and invasion.

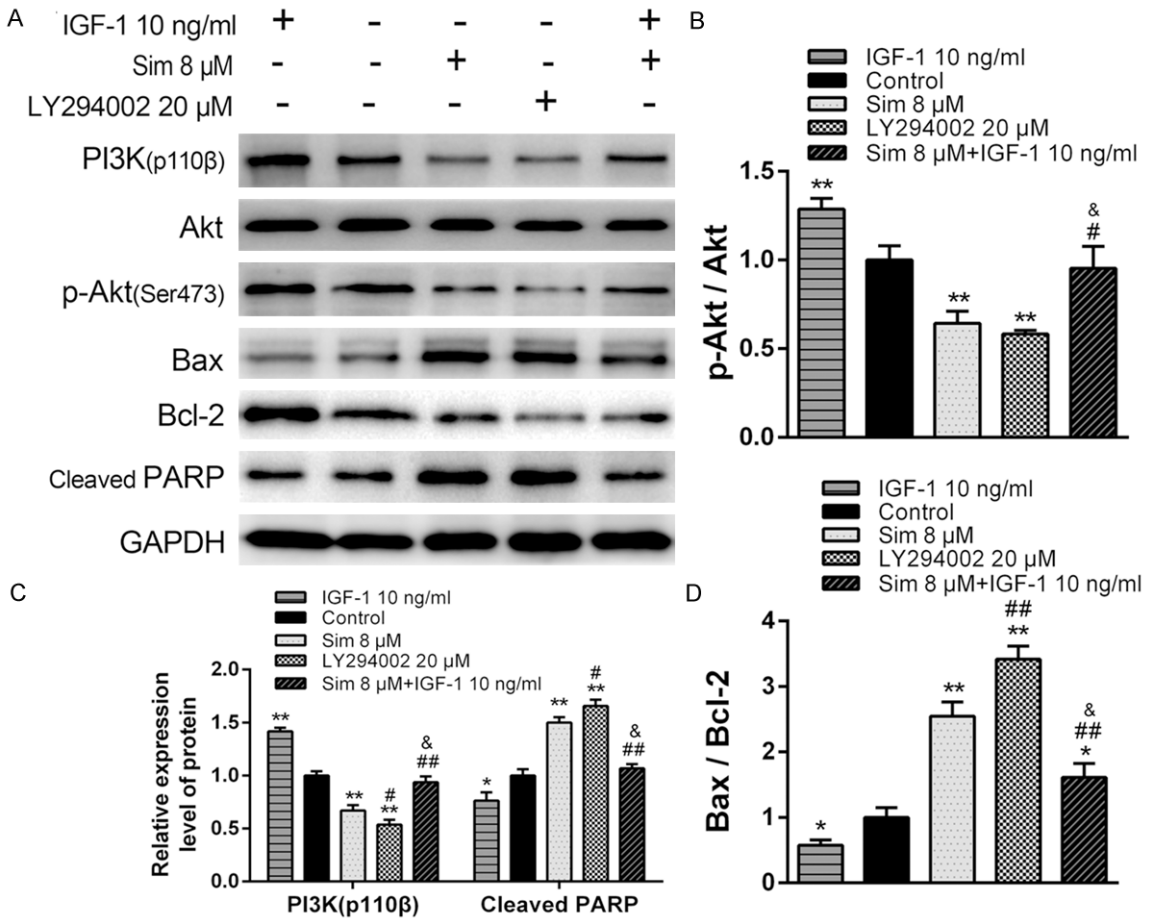

Figure 5. The Inactivation of PI3K/Akt signaling pathway was involved in Sim-induced apoptosis. The MNNG/HOS cells were pretreated with IGF-1 (10 ng/ml) for 2 h, followed by treatment with IGF-1 or co-treatment with Sim (8 μM) for 48 h. The other groups were treated with Sim (8 μM) or LY294002 (20 μM) for 48 h. Protein expressions were determined by Western blot and quantified densitometric analysis. (A) Representative blots. Relative expression levels of (C) PI3K (p110β) and cleaved PARP. The ratio of expressions of (B) p-Akt/Akt, (D) Bax/Bcl-2. GAPDH was used as a loading control. Data are expressed as the means ± SD from three independent experiments. *P<0.05, **P<0.01 vs. control groups. #P<0.05, ##P<0.01 vs. Sim groups. &P<0.05 vs. IGF-1 groups.

We further investigated the underlying molecular mechanism that might be responsible for the Sim-induced suppression of cell invasion. We determined the expression of Matrix metalloproteinases (MMPs) by Western blot. As shown in **Figure 2E** and **2F**, the protein expressions of MMP-2 and MMP-9 were markedly inhibited in a dose-dependent manner in Sim-treated cells compared with the control groups (P<0.05). Therefore, our results suggested that the down-regulation of MMP-2 and MMP-9 might be responsible for Sim-induced invasive suppression in MNNG/HOS cells.

Effects of Sim on cell cycle distribution

To further analyze the if Sim-induced growth inhibition of osteosarcoma cells was a result of induction of cell cycle arrest, flow cytometric analysis was performed to assess the cell population at various stages of cell cycle. The results revealed that Sim caused significant accumulation of cells in G0/G1 phase in a dose-dependent manner in MNNG/HOS cells (**Figure 3A** and **3B**, P<0.05). Nearly 51.2±2.8% of the cells accumulated in G0/G1 phase as compared to 34.7±2.3% in control groups at 16 μM of Sim.

To elucidate whether cell cycle arrest is associated with the regulation of cell cycle checkpoint proteins, we examined the expression of related proteins by Western blot. As some index for G1 phase arrest, we measured the expression levels of cyclin-dependent kinases (CDKs)

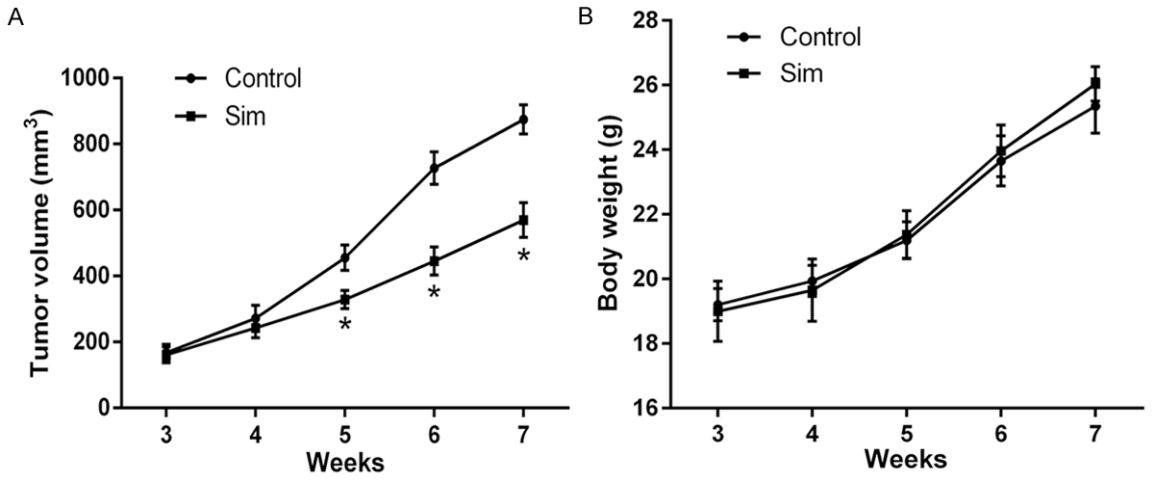

Figure 6. Sim inhibited tumor growth in osteosarcoma xenograft tumor mouse models. A. Graph representing the average tumor volumes of MNNG/HOS xenografts treated with or without Sim. B. Body weight curve of nude mice bearing MNNG/HOS tumors in Sim and control groups. Data are expressed as the means ± SD from three independent experiments. *P<0.05 vs. control groups.

CDK2, CDK4, of cyclin D1, and of cyclin-dependent kinase inhibitors (CDKIs) p21 Cip1 and p27 Kip1. As representatively demonstrated in **Figure 3C** and **3D**, MNNG/HOS cells exposed to Sim treatment for 48 h exhibited a dose-dependent decrease in cyclin D1, CDK2 and CDK4 compared with the control groups (P< 0.01). Whereas the expressions of CDKIs, p21 Cip1 and p27 Kip1, were remarkably enhanced (P<0.01). These findings coincide with the Sim-induced cell cycle arrest in the G0/G1 phase.

Sim induced cell apoptosis

The flow cytometry was used to quantify the apoptosis in MNNG/HOS cells triggered by Sim. The results showed that the apoptotic effects of Sim significantly increased in dose-dependent manner compared with control groups (**Figure 4A** and **4B**, P<0.01). The percentage of apoptotic cells (early apoptosis + late apoptosis) increased from 11.35±2.57% in control groups to 24.47±2.58% (8 μM), 38.53±2.81% (16 μM) in Sim treated cells respectively. The different quadrants differentiate necrotic cells (Annexin V-FITC -/PI +, left upper quadrant, Q1) from early apoptotic cells (Annexin V-FITC +/PI -, right lower quadrant, Q3) and late apoptotic cells (Annexin V-FITC +/PI +, right upper quadrant, Q2). Q4 quadrant shows the percentage of live cells.

Sim induced apoptosis via inactivation of PI3K/Akt pathway and enhancement of Bax/Bcl-2 expression

The PI3K/Akt signaling pathway is significant for cell existence and apoptosis. Therefore, the potential role of Sim on the PI3K/Akt signaling pathway was examined by Western blot. After the MNNG/HOS cells were treated with various concentrations of Sim (0, 8, 16 μM) for 48 h, as shown in **Figure 4C**, **4D** and **4F**, the expressions of PI3K (p110β) and phospho-Akt (p-Akt) (Ser 473) decreased significantly compared with control cells (P<0.01), while total Akt protein level were unaffected (P>0.05). We also analyzed expressions of the pro-apoptotic protein Bax, anti-apoptotic protein Bcl-2, and downstream cleaved poly (ADP-ribose) polymerase (PARP) by Western blot. Our results showed the expressions of Bax and cleaved PARP were significantly enhanced, whereas the expression of Bcl-2 was down-regulated by Sim, thus leading to an up-regulation in the ratio of Bax/Bcl-2 compared with control groups (**Figure 4C**, **4E** and **4G**, P<0.01). This may be one of the molecular mechanisms by which Sim induced apoptosis in MNNG/HOS cells.

To further test the contribution of PI3K/Akt pathway in Sim-induced apoptosis, insulin-like growth factor-1 (IGF-1), one of the most potent activators of the PI3K/Akt signaling pathway, and LY294002, a specific PI3K inhibitor, were

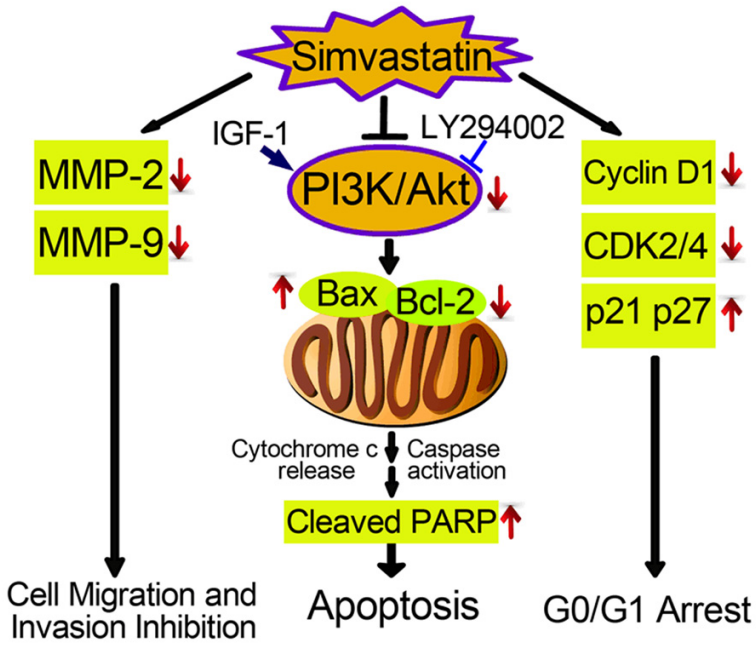

Figure 7. Proposed model of Sim induced migration and invasion inhibition, cell cycle arrest and apoptosis in human osteosarcoma MNNG/HOS cells. The arrows indicated the expression changes in our results.

used. The MNNG/HOS cells were pretreated with IGF-1 (10 ng/ml) for 2 h in order to activate the PI3K/Akt signaling pathway, followed by treatment with IGF-1 or co-treatment with Sim (8 μM) for 48 h. In other groups, the cells were treated with Sim (8 μM) for 48 h, or LY294002 (20 μM) for 48 h as a positive control [16, 17]. As can be seen in **Figure 5**, Western blot analysis indicated that IGF-1 significantly activated PI3K/Akt signaling pathway by up-regulated the expressions of PI3K (p110β), p-Akt to promote cell growth, thus the ratio of downstream Bax/Bcl-2 was enhanced and the expression of cleaved PARP was down-regulated ($P<0.05$ vs. control groups). However, the Sim treatment had a reversal of roles, even simulated partly the effects of LY294002 (20 μM) on MNNG/HOS cells by inactivation of PI3K/Akt signaling pathway. In addition, co-treated with Sim and IGF-1 almost completely reversed the IGF-1-induced up-regulation of PI3K and p-Akt ($P<0.05$), which suggested that blockage of PI3K/Akt pathway might account for Sim-induced apoptosis.

Sim suppresses the growth of osteosarcoma in vivo

To assess the effects of Sim on osteosarcoma growth in vivo, we utilized xenograft tumor mouse models by injecting MNNG/HOS cells into the flanks of nude mice and determined tumor growth and body weight of mice. During the treatment, the mice showed tolerance to Sim injections and maintained normal activities. We found that Sim significantly reduced the tumor volume compared with control mice (**Figure 6A**, $P<0.01$). Furthermore, there was no significant toxicity to mice treated with Sim by assessing mice weight of 2 groups (**Figure 6B**, $P>0.05$).

Discussion

In the present study, we showed that Sim could potently inhibit human osteosarcoma cell proliferation and mobility in vitro, induce G0/G1 phase arrest and apoptosis, and suppress tumor growth in xenograft model. Our data revealed that the possible molecular mechanisms by which Sim exerted the anticancer effects involved in alterations of MMP-2, -9, cell cycle regulators, and inactivation of PI3K/Akt signaling pathway.

Recently, Sim has been demonstrated to exert anti-tumor effects on various cancer cells of different origins. In addition, many epidemiological studies have shown a correlation between Sim use and a relative reduction in the risk of gastric, pancreatic, colorectal and prostate cancer [18-21]. In the present study, our experiments revealed that Sim inhibited the MNNG/HOS cells proliferation in culture and in vivo, which were in agreement with previous researches [8, 9, 22]. Simultaneously, we investigated the effects of Sim on biological behavior of MNNG/HOS cells, such as cell migration and invasion. As we know, tumor metastasis is a dynamic biological, multi-step and complex event, in which the matrix metalloproteinases (MMPs) are required and play crucial role [23]. Among the MMPs, MMP-2 and MMP-9 are involved with the invasive metastatic potential of tumor cells because of their capability to degrade various types of collagens [24]. Therefore, it is well-established that inhibitions

of MMP-2 and -9 proteins expression are early targets for preventing cancer metastasis. We found that Sim suppressed the MNNG/HOS cells migration and invasion in a dose-dependent manner, and the possible mechanism was involved in down-regulation of MMP-2 and MMP-9. Our results strengthen the potential use of Sim as a new strategy for anticancer therapy against migration and invasion of osteosarcoma cells.

A great number of analyses of human malignancy tumors revealed that cell cycle regulators are frequently mutated [25, 26]; therefore, targeting regulators to control cell cycle progression is an feasible alternative in cancer therapy. In the current study, Sim induced G0/G1 cell cycle arrest in MNNG/HOS cells, which was consistent with previous research in other human malignancies [8, 9, 13]. Furthermore, to analyze the underlying biological mechanisms in Sim-induced G0/G1 cell cycle arrest in MNNG/HOS cells, proteins expressions including cyclins, CDKs and CDKIs were determined. Our results revealed that Sim-induced G0/G1 cell cycle arrest were associated with a marked reduction of cyclin D1, CDK2 and CDK4 as well as up-regulation of p21 and p27. As is known, cell cycle progression is regulated by CDKs and CDKIs whose activities are highly controlled and coordinated by cyclins. Cyclin D-CDK2/4 complexes are the primary regulators and required for the cell cycle G1/S transition [27]. The p21 and p27 gene, which recently been discovered to be important CDKIs, are all candidate tumor suppressor genes whose function as a regulator of cell cycle progression at the G1 phase [28]. Our finding involved the possible mechanism of Sim-induced G0/G1 phase arrest in MNNG/HOS cells is the first report by now.

Many recently published reports suggested that Sim exerted anti-cancer effects by inducing apoptosis via down-regulation of critical signaling pathways in a few human cancers, including MAPK, Akt/mTOR, JAK2/STAT3 signaling pathways [8-10]. Our results showed that Sim was capable of triggering apoptosis in MNNG/HOS cells in a dose-dependent manner by down-regulation of PI3K/Akt axis. The PI3K/Akt signaling pathway, a well-established and crucial signal transduction pathway, plays critical roles in suppressing apoptosis and promoting cell proliferation by affecting the activation state of a range of downstream effector molecules [29]. Thus, blocking this pathway or targeting the downstream substrates, for instance Bcl-2 and Bax, was a favorable strategy for the development of novel approaches in cancer therapy. Bcl-2 and Bax, the important members of Bcl-2 gene families, take important parts in the functional regulation of cell apoptosis by altering mitochondrial permeability transition [30]. The induction of Bax is associated with the release of cytochrome c from the mitochondria to the cytosol and the cleavage of PARP [31]. To further confirm whether the apoptosis of MNNG/HOS cells induced by Sim was mainly regulated through the PI3K/Akt pathway, IGF-1 and LY294002 were used to activate or inactivate this pathway for evaluating the underlying mechanisms. Recent studies indicate that IGF-1 not only acts as an activator of PI3K, but also involves in cellular processes such as protection from apoptosis and promotion of proliferation via Akt activation [32]. It was noteworthy that in addition to inhibition of Akt activity, Sim treatment can partly approach the efficacy of LY294002 and acted as an inhibitor of PI3K/Akt axis. Furthermore, Sim completely reversed IGF-1-induced activation of PI3K/Akt pathway highlighted the possibly mechanisms that Sim-induced apoptosis in MNNG/HOS cells was involved in inactivation of PI3K/Akt signaling pathway.

In conclusion, the current study demonstrated that Sim inhibited osteosarcoma cell proliferation in culture and tumor growth in vivo. Sim suppressed MNNG/HOS cells migration and invasion by down-regulation of expressions of MMP-2 and -9. Sim exerted the anti-tumor effects on MNNG/HOS cells by inducing G0/G1 phase arrest and apoptosis, the possible mechanism was involved in alterations of cell cycle regulators and inactivation of PI3K/Akt signaling pathway (**Figure 7**). Our novel findings shed new light on the possibility of Sim as a tumor suppressor for human osteosarcoma treatment.

Acknowledgements

This study was supported by the National Natural Scientific Foundation of China (81172551) and Science Foundation of Qilu Hospital of Shandong University and the Fundamental Research Funds of Shandong University (2015-QLQN34).

Disclosure of conflict of interest

None.

Address correspondence to: Dr. Jianmin Li, Department of Orthopedics, Qilu Hospital, Shandong University, 107 Wenhuaxi Road, Ji'nan 250012, Shandong, China. Tel: (+86) 531-82166541; Fax: (+86) 531-82949227; E-mail: drgkljm@163.com

References

[1] Botter SM, Neri D and Fuchs B. Recent advances in osteosarcoma. Curr Opin Pharmacol 2014; 16: 15-23.

[2] Bielack SS, Kempf-Bielack B, Delling G, Exner GU, Flege S, Helmke K, Kotz R, Salzer-Kuntschik M, Werner M, Winkelmann W, Zoubek A, Jurgens H and Winkler K. Prognostic factors in high-grade osteosarcoma of the extremities or trunk: an analysis of 1,702 patients treated on neoadjuvant cooperative osteosarcoma study group protocols. J Clin Oncol 2002; 20: 776-790.

[3] Baigent C, Keech A, Kearney PM, Blackwell L, Buck G, Pollicino C, Kirby A, Sourjina T, Peto R, Collins R and Simes R. Efficacy and safety of cholesterol-lowering treatment: prospective meta-analysis of data from 90,056 participants in 14 randomised trials of statins. Lancet 2005; 366: 1267-1278.

[4] Crescencio ME, Rodriguez E, Paez A, Masso FA, Montano LF and Lopez-Marure R. Statins inhibit the proliferation and induce cell death of human papilloma virus positive and negative cervical cancer cells. Int J Biomed Sci 2009; 5: 411-420.

[5] Liu H, Liang SL, Kumar S, Weyman CM, Liu W and Zhou A. Statins induce apoptosis in ovarian cancer cells through activation of JNK and enhancement of Bim expression. Cancer Chemother Pharmacol 2009; 63: 997-1005.

[6] Mistafa O and Stenius U. Statins inhibit Akt/PKB signaling via P2X7 receptor in pancreatic cancer cells. Biochem Pharmacol 2009; 78: 1115-1126.

[7] Gbelcova H, Lenicek M, Zelenka J, Knejzlik Z, Dvorakova G, Zadinova M, Pouckova P, Kudla M, Balaz P, Ruml T and Vitek L. Differences in antitumor effects of various statins on human pancreatic cancer. Int J Cancer 2008; 122: 1214-1221.

[8] Stine JE, Guo H, Sheng X, Han X, Schointuch MN, Gilliam TP, Gehrig PA, Zhou C and Bae-Jump VL. The HMG-CoA reductase inhibitor, simvastatin, exhibits anti-metastatic and anti-tumorigenic effects in ovarian cancer. Oncotarget 2016; 7: 946-60.

[9] Lee J, Hong EM, Jang JA, Park SW, Koh DH, Choi MH, Jang HJ and Kae SH. Simvastatin Induces Apoptosis and Suppresses Insulin-Like Growth Factor 1 Receptor in Bile Duct Cancer Cells. Gut Liver 2016; 10: 310-7.

[10] Fang Z, Tang Y, Fang J, Zhou Z, Xing Z, Guo Z, Guo X, Wang W, Jiao W, Xu Z and Liu Z. Simvastatin inhibits renal cancer cell growth and metastasis via AKT/mTOR, ERK and JAK2/STAT3 pathway. PLoS One 2013; 8: e62823.

[11] Goc A, Kochuparambil ST, Al-Husein B, Al-Azayzih A, Mohammad S and Somanath PR. Simultaneous modulation of the intrinsic and extrinsic pathways by simvastatin in mediating prostate cancer cell apoptosis. BMC Cancer 2012; 12: 409.

[12] Relja B, Meder F, Wilhelm K, Henrich D, Marzi I and Lehnert M. Simvastatin inhibits cell growth and induces apoptosis and G0/G1 cell cycle arrest in hepatic cancer cells. Int J Mol Med 2010; 26: 735-741.

[13] Liang YW, Chang CC, Hung CM, Chen TY, Huang TY and Hsu YC. Preclinical Activity of Simvastatin Induces Cell Cycle Arrest in G1 via Blockade of Cyclin D-Cdk4 Expression in Non-Small Cell Lung Cancer (NSCLC). Int J Mol Sci 2013; 14: 5806-5816.

[14] Liu XN, Wang S, Yang Q, Wang YJ, Chen DX and Zhu XX. ESC reverses epithelial mesenchymal transition induced by transforming growth factor-beta via inhibition of Smad signal pathway in HepG2 liver cancer cells. Cancer Cell Int 2015; 15: 114.

[15] Li Y, Zhang J, Zhang L, Si M, Yin H and Li J. Diallyl trisulfide inhibits proliferation, invasion and angiogenesis of osteosarcoma cells by switching on suppressor microRNAs and inactivating of Notch-1 signaling. Carcinogenesis 2013; 34: 1601-1610.

[16] Yamaguchi K, Lee SH, Kim JS, Wimalasena J, Kitajima S and Baek SJ. Activating transcription factor 3 and early growth response 1 are the novel targets of LY294002 in a phosphatidylinositol 3-kinase-independent pathway. Cancer Res 2006; 66: 2376-2384.

[17] Samani AA, Yakar S, LeRoith D and Brodt P. The role of the IGF system in cancer growth and metastasis: overview and recent insights. Endocr Rev 2007; 28: 20-47.

[18] Mucci LA and Stampfer MJ. Mounting evidence for prediagnostic use of statins in reducing risk of lethal prostate cancer. J Clin Oncol 2014; 32: 1-2.

[19] Cai H, Zhang G, Wang Z, Luo Z and Zhou X. Relationship between the use of statins and patient survival in colorectal cancer: a systematic review and meta-analysis. PLoS One 2015; 10: e0126944.

[20] Chen MJ, Tsan YT, Liou JM, Lee YC, Wu MS, Chiu HM, Wang HP and Chen PC. Statins and the risk of pancreatic cancer in Type 2 diabetic patients-A population-based cohort study. Int J Cancer 2016; 138: 594-603.
[21] Lin CJ, Liao WC, Lin HJ, Hsu YM, Lin CL, Chen YA, Feng CL, Chen CJ, Kao MC, Lai CH and Kao CH. Statins Attenuate Helicobacter pylori CagA Translocation and Reduce Incidence of Gastric Cancer: In Vitro and Population-Based Case-Control Studies. PLoS One 2016; 11: e0146432.
[22] Kochuparambil ST, Al-Husein B, Goc A, Soliman S and Somanath PR. Anticancer Efficacy of Simvastatin on Prostate Cancer Cells and Tumor Xenografts Is Associated with Inhibition of Akt and Reduced Prostate-Specific Antigen Expression. J Pharmacol Exp Ther 2011; 336: 496-505.
[23] Jacob A and Prekeris R. The regulation of MMP targeting to invadopodia during cancer metastasis. Front Cell Dev Biol 2015; 3: 4.
[24] Wang R, Ke ZF, Wang F, Zhang WH, Wang YF, Li SH and Wang LT. GOLPH3 overexpression is closely correlated with poor prognosis in human non-small cell lung cancer and mediates its metastasis through upregulating MMP-2 and MMP-9. Cell Physiol Biochem 2015; 35: 969-982.
[25] Kastan MB, Canman CE and Leonard CJ. P53, cell cycle control and apoptosis: implications for cancer. Cancer Metastasis Rev 1995; 14: 3-15.
[26] Molinari M. Cell cycle checkpoints and their inactivation in human cancer. Cell Prolif 2000; 33: 261-274.
[27] Murray AW. Recycling the cell cycle: cyclins revisited. Cell 2004; 116: 221-234.
[28] Karimian H, Moghadamtousi SZ, Fadaeinasab M, Golbabapour S, Razavi M, Hajrezaie M, Arya A, Abdulla MA, Mohan S, Ali HM and Noordin MI. Ferulago angulata activates intrinsic pathway of apoptosis in MCF-7 cells associated with G1 cell cycle arrest via involvement of p21/p27. Drug Des Devel Ther 2014; 8: 1481-1497.
[29] Zhang J, Yu XH, Yan YG, Wang C and Wang WJ. PI3K/Akt signaling in osteosarcoma. Clin Chim Acta 2015; 444: 182-192.
[30] Li H, Li X, Bai M, Suo Y, Zhang G and Cao X. Matrine inhibited proliferation and increased apoptosis in human breast cancer MCF-7 cells via upregulation of Bax and downregulation of Bcl-2. Int J Clin Exp Pathol 2015; 8: 14793-14799.
[31] Wang Y, Yin RF and Teng JS. Wogonoside induces cell cycle arrest and mitochondrial mediated apoptosis by modulation of Bcl-2 and Bax in osteosarcoma cancer cells. Int J Clin Exp Pathol 2015; 8: 63-72.
[32] Yu M, Wang H, Xu Y, Yu D, Li D, Liu X and Du W. Insulin-like growth factor-1 (IGF-1) promotes myoblast proliferation and skeletal muscle growth of embryonic chickens via the PI3K/Akt signalling pathway. Cell Biol Int 2015; 39: 910-922.